Journal of Building Engineering 41 (2021) 102776

Contents lists available at ScienceDirect

Journal of Building Engineering

journal homepage: www.elsevier.com/locate/jobe

Experimental investigations on the structural behaviour of reinforced geopolymer beams produced from recycled construction materials

Şaban Akduman [a], Oznur Kocaer [a], Alper Aldemir [a,*], Mustafa Şahmaran [a], Gürkan Yıldırım [a], Hanady Almahmood [b], Ashraf Ashour [b]

[a] Hacettepe University, Department of Civil Engineering, Ankara, Turkey
[b] University of Bradford, Department of Civil and Structural Engineering, Bradford, United Kingdom

ARTICLE INFO

Keywords:
Recycled aggregate
Geopolymer concrete
Bending tests
Recycled construction materials
Flexural behaviour

ABSTRACT

Concrete requires a vast amount of aggregate and cement production. Although there are some efforts in the literature to reduce the amount of Portland cement in the concrete mixture to lessen the greenhouse gas release, a limited number of studies were conducted to investigate the possibility of using this geopolymer mixtures to serve as a structural component. Therefore, this study firstly aimed to produce geopolymer concrete from construction and demolition waste-based precursors, including masonry units (red clay brick, roof tile, hollow brick, etc.) and glass. In addition, recycled aggregates produced from the concrete waste portion of the CDW were used to obtain 100% recycled construction material on the scale of the binder and aggregate phase. Then, this study investigated the possible use of this proposed geopolymer concrete to produce structural components that perform similar to conventional concrete. Therefore, the structural properties of reinforced geopolymer concrete beams produced from the recycled construction demolition wastes were evaluated in this study by conducting laboratory experiments. To this end, bending tests were performed on reinforced conventional concrete beam specimens and reinforced geopolymer concrete beam specimens. The test observations clearly showed that construction demolition waste could be recycled to produce new constructional components, considering its advantage of promoted sustainability.

1. Introduction

The excess of waste generated in the industry is a concern for environmental health. In this respect, utilizing the wastes in concrete are of great importance. By replacing a certain amount of cement or aggregate with waste products, it is aimed to increase the sustainability of concrete and reduce the damage to the environment [1]. Although concrete is one of the most widely used construction materials in the world, there exist some environmental and structural disadvantages related to its sustainability. The main component of concrete is the Portland cement, whose production reaches billions of tons each year and responsible for 7% of human-induced carbon dioxide emissions [11–19]. For instance, approximately 1.5 tons of raw materials are required to produce 1 ton of Portland cement, emitting nearly 1 ton of carbon dioxide [1–12]. In addition, the production stages of the Portland cement require a high level of input energy. Considering the growth levels of emerging economies from day to day and the exponential increase in construction/renovation demand for infrastructures, it is expected that the greenhouse gas emissions and energy consumption arising from the production of cement will reach 105 Gt (gigatonne) and 505 TJ (terajoule) in 30 years, respectively [20]. Besides, increasing aggregate production in proportion to the demand for concrete is another concern to overcome due to adverse environmental impact. The carbon dioxide emissions derived by aggregate production are responsible for 20% of the emitted carbon dioxide by concrete [21]. Therefore, it is apparent that the extensive use of conventional concrete is not sustainable with its all components. For this reason, the development of eco-friendly, cost-effective, and low-carbon-footprint construction materials should become a forefront priority worldwide.

In addition to the environmental damages caused by conventional building materials, the repair and/or demolition and reconstruction of the infrastructure systems before completing their service life, due to the

* Corresponding author.
E-mail addresses: akduman501@gmail.com (Ş. Akduman), oznurkocaer@hacettepe.edu.tr (O. Kocaer), alperaldemir@hacettepe.edu.tr (A. Aldemir), sahmaran@hacettepe.edu.tr (M. Şahmaran), gurkanyildirim@hacettepe.edu.tr (G. Yıldırım), h.a.a.almahmood@bradford.ac.uk (H. Almahmood), a.f.ashour@bradford.ac.uk (A. Ashour).

https://doi.org/10.1016/j.jobe.2021.102776
Received 9 March 2021; Received in revised form 20 May 2021; Accepted 20 May 2021
Available online 29 May 2021

weakness of these materials in terms of sustainability, causes harmful consequences for the national economies. All the operations carried out to extend the infrastructure systems' service life or reconstruction result in vast construction and demolition waste. While the amount of CDW reached 569.4 million tons in the USA in 2017 [22], it is expected that the annual increase rate of CDW for China will reach millions in the coming years [23]. Besides the detrimental financial impact of CDW, concerns including the use of agricultural lands as waste storage areas and the toxic waste components of CDW posing a danger to the environment and human health have compelled CDW regulation.

In this context, geopolymer binders produced by activating aluminosilicate sourced raw materials using alkali activators are in a promising position in terms of being an alternative to ordinary Portland cement (OPC) in recent years. Geopolymer binders stand out by making possible lower carbon emissions levels, at least 50% lower than conventional cement-based binders, also ensures superior mechanical and durability properties [10,20,24]. Life Cycle Assessments on geopolymer binders produced using CDW or recycling of CDW to replace raw materials in different phases indicate that environmental impacts have remained relatively lower against conventional cementitious binders [25–28]. Cement-based materials generally have low tensile strength, limited ductility, and brittle behavior in the absence of proper reinforcement detailing. However, their high compressive strength, temperature and acid resistance and durability and, low cost could be considered the main reasons for the domination of conventional concrete in the construction market [6–16]. Geopolymers are members of the inorganic polymer family. They show fast chemical reactions on Si–Al minerals under alkaline conditions with a three-dimensional polymeric chain and ring structure consisting of Si–O–Al–O bonds [18,19]. Materials containing silicon and aluminum in their activator structure (e.g., fly ash, slag, rice ash, etc.) react with additives such as brass ash and produce binders [13–15]. The main difference between geopolymer concrete (GPC) and conventional concrete (CVC) is the used binder in their mixture (i.e., alkali active aluminosilicate) [6]. Geopolymer concrete is obtained by using activated pozzolanic materials and aggregates instead of cement [10]. Besides, the enhanced alkalinity of the obtained geopolymer concrete provides corrosion resistance. With its resistance to sulfate and chloride carbonation environments, geopolymer concrete shows superior properties to conventional concrete [18,19,29,30].

In recent studies [2–7], the mechanical behavior of geopolymer concrete, its durability, and the effects of different by-products used were evaluated. It was stated that GPC was a promising candidate for conventional concrete in terms of both strength and durability [31–34]. In addition, the carbon footprint of geopolymer concrete can be reduced up to 80–90%, by optimizing the alkali activators and binder content, compared to conventional concrete as it comprises industrial wastes such as fly ash, slag, glass powder, etc. [9,10,30,31]. However, studies on the use of geopolymer concrete in structural components are limited [10,34–37]. Raj et al. [38] determined the behavior of geopolymer concrete joints and compared the performance of geopolymer joints with the conventional concrete joints. They concluded that the geopolymer joints with proper steel of fiber reinforcements could behave better under cyclic loading. Ahmed et al. [39] examined the behavior of geopolymer beams reinforced with glass fiber-reinforced polymer (GFRP) bars. In this study, it was shown that the stiffness of geopolymer beams was detected to be slightly less than the conventional concrete beams, but both types of beams had approximately the same value of the ultimate load. In another study conducted by Sumajouw et al. [40], the results of experimental research and numerical analysis on the behavior and the strength of reinforced geopolymer concrete slender columns. They tested twelve columns with different longitudinal reinforcement ratios under different axial load ratios. They concluded that heat-cured low-calcium fly ash-based geopolymer concrete had excellent potential for applications in the pre-cast industry as the tests showed similar behavior with the conventional concrete counterpart. In addition, Wu et al. [41] conducted shear tests on reinforced slag-based geopolymer concrete beams with transverse reinforcement. The test parameters were the concrete type, concrete strength, longitudinal reinforcement ratio, longitudinal bar strength, shear-span-to-depth ratio, and beam depth. Wu et al. [41] concluded that the shear strength and failure modes of GPC beams were comparable to those of RC beams. Mathew and Joseph [42] investigated the effect of elevated temperatures on the flexural performance of geopolymer beams produced from low calcium fly ash. They found that the deformation characteristics of reinforced geopolymer concrete beams at ambient temperature are similar to that of the reinforced cement concrete beams. However, the ductility of the geopolymer concrete beams reduces rapidly with the increase in exposure temperature. Unlike these researches, in this study, the flexural behavior of beams produced from geopolymer concrete with 100% recycled construction material was determined to unveil the possibility to eliminate the CO_2-gas emission due to aggregate and cement production and to enhance the recycling rate in the construction practice.

To the best of the authors' knowledge, previous studies focused mainly on the structural properties of components made of geopolymer concrete produced from fly ash with no or a limited amount of recycled materials in the concrete mixture. Therefore, in this study, geopolymer concrete was produced from construction and demolition waste-based precursors, including masonry units (red clay brick, roof tile, hollow brick, etc.) and glass. In addition, recycled aggregates produced from the concrete waste portion of the CDW were used to obtain 100% recycled construction material on the scale of the binder and aggregate phase. As a result of the research team's extensive preliminary studies on optimizing the physical and chemical properties of CDW-based raw materials from different sources, a general mixture ratio for binder and activator combinations/concentrations were determined to produce geopolymer concrete with the targeted mechanical performance. The effect of the inclusion of recycled aggregate in the concrete mixture is also examined, to the best of the authors' knowledge, for the first time in the literature. Besides, recycling aggregates obtained from CDW were not subjected to any treatment to improve their mechanical properties. All the geopolymer concrete beam specimens were cured at ambient temperature. For each geopolymer concrete mixture, the flexural behavior was determined by conducting the four-point-bending test under displacement-controlled loading protocol. To this end, 150 × 250 × 1100 mm beam specimens (i.e., ½ scaled beams) were produced with code-conforming lateral reinforcement detailing. In each test, the load-midspan displacement curve, moment-curvature curve, and observed crack patterns were obtained. To investigate the effect of shear-span-to-depth ratio (a/d) on the flexural behavior, three different shear-span-to-depth ratio values for each material type were used, which corresponds to a total number of 12 tests. Therefore, the flexural behavior of CDW-based recycled geopolymer concrete was obtained.

2. Materials and methods

2.1. Details of CDW-based GPC

GPC mixtures were designed based on extensive preliminary studies conducted to develop the geopolymer phase. In this context, the precursor phase of the geopolymer binders was obtained by applying the selective demolition procedure of the inert concrete (CW), clay originated brick elements as red clay brick (RCB), hollow brick (HB), roof tile (RT), and glass (GW) part of construction and demolition waste. All these CDW-based materials are clay-based except for inert concrete materials and glass. Visuals of CDW-based precursors taken by using a digital camera and by scanning electron microscopy (SEM) are presented in Fig. 1. The chemical compositions of CDW elements were determined via X-ray fluorescence (XRF) analysis and are summarized in Table 1. These precursors were subjected to a non-complex pre-crushing and subsequent grinding, making them suitable for polymerization reactions and reducing their particle size to cement fineness (i.e.,

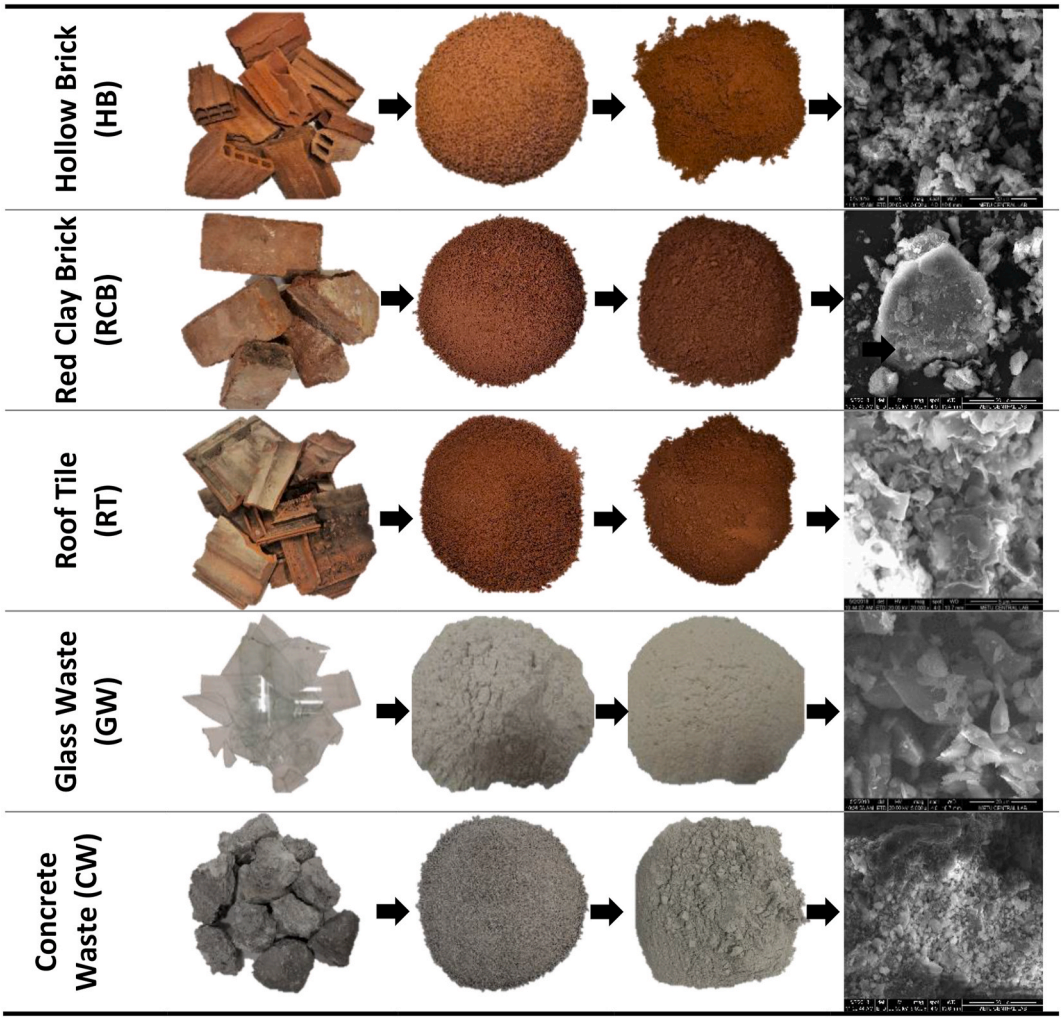

Fig. 1. Visuals of CDW-based precursors (from left to right; raw state, crushed state, ground state, SEM micrograph).

Table 1
Chemical compositions of CDW-based precursors.

Oxides, %	Hollow Brick (HB)	Red Clay Brick (RCB)	Roof Tile (RT)	Glass Waste (GW)	Concrete Waste (CW)
SiO_2	39.7	41.7	42.6	66.5	31.6
Al_2O_3	13.8	17.3	15.0	0.9	4.8
Fe_2O_3	11.8	11.3	11.6	0.3	3.5
CaO	11.6	7.7	10.7	10.0	31.3
Na_2O	1.5	1.2	1.6	13.6	5.1
MgO	6.5	6.5	6.3	3.9	0.9
SO_3	3.4	1.4	0.7	0.2	0.5
K_2O	1.6	2.7	1.6	0.2	0.7
TiO_2	1.7	1.6	1.8	0.1	0.2
P_2O_5	0.3	0.3	0.3	0.0	0.1
Cr_2O_3	0.1	0.1	0.1	0.0	0.1
Mn_2O_3	0.2	0.2	0.2	0.0	0.1

maximum size less than 100 μm). The primary objective of the simple procedure for processing precursors is to reduce the amount of energy consumption and labor. Given the variability of CDW elements and the fact that all CDW elements can be collected at a construction/demolition site in a batch, a consistent milling period is critical to ensure that separated and non-separated CDW elements have similar particle sizes. As a result of the preliminary studies carried out in this context, the materials were reduced to their final particle size during the 1-h grinding period determined for the binder phase to reach a particle size of fewer than 100 μm. Particle size distributions of CDW-based precursors are given in Fig. 2. The aggregate phase of GPC mixtures was obtained by subjecting concrete waste obtained from construction and demolition waste (CDW) only to the pre-crushing process and separating the different particle size ranges by using sieves with various openings. In the production of geopolymer concrete, the maximum recycling aggregate size is determined to be $D_{max} = 16$ mm in line with the particle size distribution Fuller-Thompson ideal gradation curve (Fig. 3). Recycling aggregates obtained from CDW were not subjected to any procedures for their improvements.

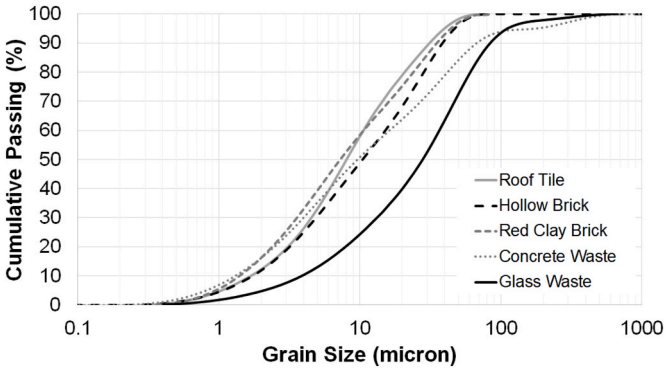

Fig. 2. Particle size distribution of CDW-based precursors.

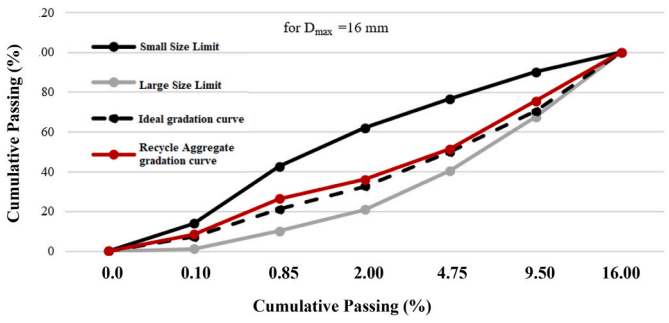

Fig. 3. Granulometry analysis of Recycled Aggregates.

Another essential element for the preparation of GPC mixtures is the type and concentration of alkaline activators. Three different activators were tested by activating the binding phase at different concentrations and in various combinations to determine the activator's types and phases in question. The mixtures with the highest mechanical performance formed the basis of the GPC mixtures. Calcium hydroxide, sodium hydroxide, and sodium silicate have been used as activators in mixtures as their alkaline properties and capability to ensure a high power of hydrogen (pH) medium to provide the geopolymerization reactions. As a result of extensive studies carried out to determine the alkali activator combination, the molar concentration of sodium hydroxide was selected as 8 M. In contrast, the sodium silicate was chosen to be two times the sodium hydroxide amount by weight. Calcium hydroxide was added to the mixtures as 5% of the total binder amount. Considering the properties such as water absorption, porosity, adherent cement particle content of the existing fine aggregates in the scope of CDW-based recycling aggregates that form the aggregate phase of GPC concrete mixtures, different gradations and different binder/aggregate ratios are tested at a 1/1 binder/aggregate ratio determined as a result of extensive preliminary studies [5,6]. The details on the geopolymer concrete compositions could be found in the recent studies conducted by Yildirim et al. [5] and Ulugöl et al. [6]. The production of geopolymer concrete samples was carried out by a simple mixing operation. The sodium hydroxide solution, which was prepared 24 h before the mixing operation, was added to the mixture of binder powder, calcium hydroxide, and aggregate phase, which was mixed for 5 min in a dry state to ensure homogeneous distribution, while the mixing operation was continued. Afterward, sodium silicate in liquid form was added to the mixing slowly; then, the operation was completed after an additional mixing for 15 min.

2.2. Other mixtures

In this study, control specimens were also produced to compare the performance of the GPC (GPC-NA) and GPC with recycled aggregates (GPC-RA). Thus, four different mixtures were prepared: GPC-NA, GPC-RA, conventional concrete with normal aggregates (CVC-NA), and conventional concrete with recycled aggregates (CVC-RA). The only difference between GPC-NA (CVC-NA) and GPC-RA (CVC-RA) is the inclusion of replacement of normal aggregates with recycled aggregates. The other components of the mixtures are kept the same. The details of mixtures for GPC and CVC specimens are presented in Table 2.

3. Beam specimens, testing, and instrumentation

The geometrical and reinforcement details of the tested specimen were selected from the first-story central-internal bay of the three-story prototype RC building designed according to the Turkish Earthquake Code (TEC2018 [43]). The cross-section of the test beam was 150 × 250 mm. A similar procedure to determine the inelastic performance of RC structural members in the literature was followed in this study [44–48].

Table 2
The content of the geopolymer concrete and concrete mixtures.

Ingredients	Masses in Geopolymer Concrete (kg/m^3)	Masses in Conventional Concrete (kg/m^3)
Red Clay Brick	150	–
Hollow Brick	200	–
Roof Tile	250	–
Glass	100	–
Recycled Concrete	100	–
Cement	–	316
Slag	200	–
Fly Ash	50	–
$Ca(OH)_2$	50	–
NaOH	112	–
Na_2SiO_3	224	–
Fine Aggregate	250	917
Coarse Aggregate	750	917
Water	200	211
Water/Binder	0.19	0.67

Fine and coarse aggregates have been used in the production of geopolymer concrete. The maximum aggregate size (MAS) was selected as 10 mm in order not to violate the laws of similitude [49,50] since the MAS of the prototype CVC was 20 mm. In other words, the scaling process was aimed to generate the same stress demands on both the prototype and the scaled specimens but the fracture energy of the prototype and scaled concrete mixtures should be the same for accurate testing [50]. Saouma et al. [51] proved that the fracture energy of the concrete was inversely proportional to the fracture process zone, which could be reduced to its half value by scaling down the aggregate size [50,51]. To this end, MAS was also reduced by the selected scale factor during the specimen production. The target compressive strength was selected as 35 MPa. The average uniaxial cylinder compressive strength and the average splitting tensile strength of the test specimens are given in Table 3 (i.e., 150 × 300 mm cylinders). In Table 3, the standard deviations of each test were also presented. It is apparent that the GPC mixtures had larger standard deviations compared to CVC mixtures. The

Table 3
Summary of test specimens.

Specimens	Shear-span/ Depth	Concrete Compressive Strength (MPa)	Concrete Splitting Tensile Strength (MPa)
CVC-NA-0.50	0.50	34.10 (1.32)[a]	2.45 (0.15)[a]
CVC-NA-1.00	1.00		
CVC-NA-1.65	1.65		
CVC-RA-0.50	0.50	35.20 (1.60)	2.21 (0.17)
CVC-RA-1.00	1.00		
CVC-RA-1.65	1.65		
GPC-NA-0.50	0.50	37.50 (2.83)	2.56 (0.29)
GPC -NA-1.00	1.00		
GPC -NA-1.65	1.65		
GPC-RA-0.50	0.50	36.60 (2.06)	2.37 (0.31)
GPC -RA-1.00	1.00		
GPC -RA-1.65	1.65		

[a] Numbers in parentheses are standard deviations.

yield and ultimate strength of the 10 mm (6.5 mm) bars were 456 MPa (330 MPa) and 716 MPa (449 MPa), respectively. Tie spacing was 100 mm over the beam length. All the ties were anchored to the core using 135° hooks to simulate code-compliant detailing.

Three different concrete shear-span-to-depth (a/d) ratios (i.e., 0.50, 1.00, and 1.65) were used in the testing program to observe the change in the failure pattern depending on the critical loading effects (i.e., shear-dominant behavior and flexure-dominant behavior). The beam specimens have the same reinforcement arrangements to examine the impact of the application of the geopolymer concrete and the recycled aggregate on the performance. All the reinforcement details are in compliance with the current seismic code in Turkey (i.e., TEC2018 [43]). The details of reinforcements used for all specimens are given in Fig. 4. In addition, a schematic of all variables and all methods considered in the scope of this study was prepared for clarity (Fig. 5).

The test setup is shown in Fig. 4. Vertical loads were applied by a displacement-controlled hydraulic actuator. The universal testing system had a loading capacity of 40 tons. The testing equipment was designed to represent a closed system, eliminating the strong base anchorages of the system to the RC slab. It was equipped with an electrohydraulic servo valve with a displacement application rate range of 0.10–1 mm/min. The accuracy of the test was ±0.5%. The tests in this study were performed with a constant displacement rate of 0.30 mm/min. All specimens were tested under a four-point loading system, i.e., subjected to two-point loads and supported on pin supports at both ends. The clear span of each specimen was 1000 mm. For all specimens, applied vertical forces were monitored with a load cell. The midspan vertical displacement was measured using Linear Variable Differential Transformers (LVDTs) placed at the center of the beam. The average curvature response of all specimens was also determined by placing lateral LVDTs (Fig. 4). Lateral LVDTs were placed in beam specimens at 100-mm, 50-mm, and 100-mm intervals for left span, midspan, and right span, respectively (Fig. 4). The accuracy of each LVDT was ±0.1%. All beam specimens were tested under a four-point bending test shown in Fig. 4. Load deflection curves, moment-curve curves, and crack patterns were determined to compare the performance of geopolymer concrete.

4. Results

In this section, the test results and the observed crack patterns during each experiment were documented. To this end, the vertical load-midspan displacement and the moment-curvature responses of all specimens are drawn and compared with different materials for a constant a/d ratio. For the sake of clarity, the ultimate force (F_u), ultimate displacement (u_u: displacement corresponding to the end of the test or the 20% capacity drop), the yield force, and displacement (F_y and u_y determined by using the bilinearization procedure in FEMA356 [52]), the displacement ductility (μ_u: u_u/u_y), the ultimate curvature (φ_u: curvature corresponding to the end of the test or the 20% capacity drop), the yield curvature (φ_y: yield curvature determined by using the bilinearization procedure in FEMA356 [52]), the curvature ductility (μ_φ: φ_u/φ_y), the energy dissipation capacity (E_t) and the normalized energy capacity (E_n: $E_t/(F_y \times u_y/2)$) measured during the tests are tabulated. The damage photographs at different displacement levels are also presented. It should be noted that only one test was performed for each selected a/d ratio for all mixtures. The compressive strength and splitting tensile strength of each specimen were determined on the test day. Average strengths and their standard deviations are presented in Table 3.

4.1. Test results of beam specimens with a/d = 0.50

The total vertical load-midspan displacement and the moment-curvature responses of CVC-NA-0.50, CVC-RA-0.50, GPC-NA-0.50, and GPC-RA-0.50 are given in Fig. 6. It could easily be inferred from Fig. 6 that the response of all specimens is brittle. Limited or no post-yield response was observed. This observation was also validated by the determined crack patterns (Fig. 7). It is apparent from Fig. 7 that all specimens failed by a shear – crack reaching the support. The yield and ultimate loads, yield and ultimate displacements, as well as the ductility indices, are presented in Table 4.

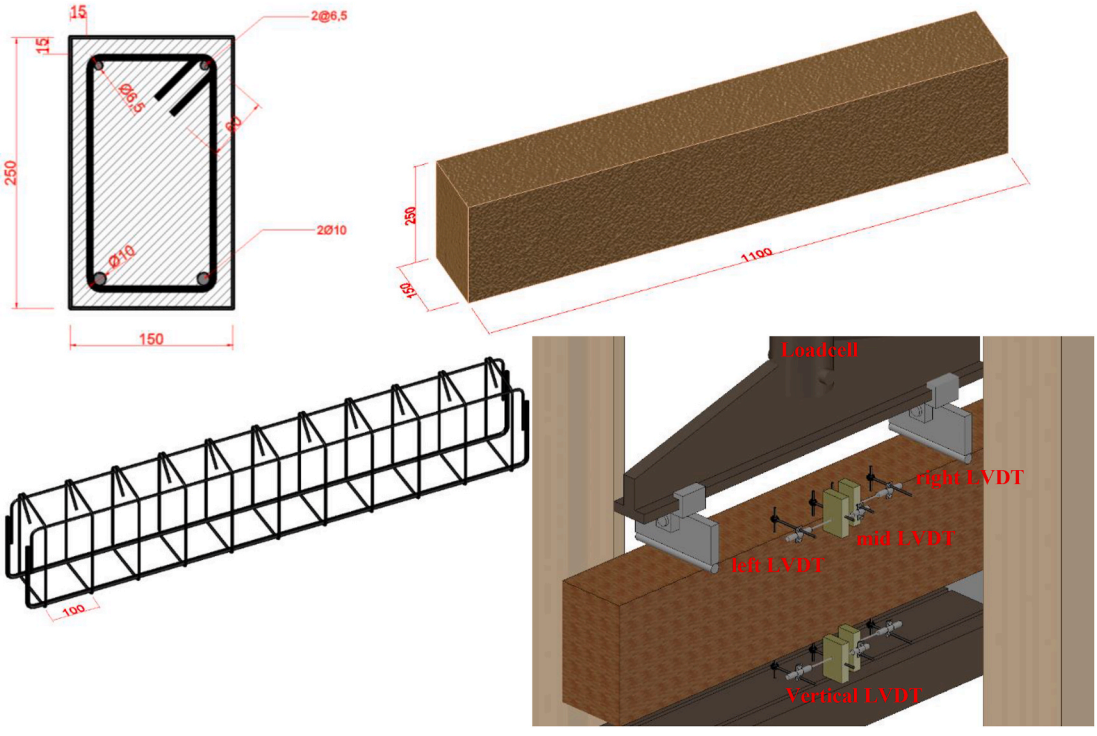

Fig. 4. Details on reinforcement and instrumentation. *All dimensions are given in mm.

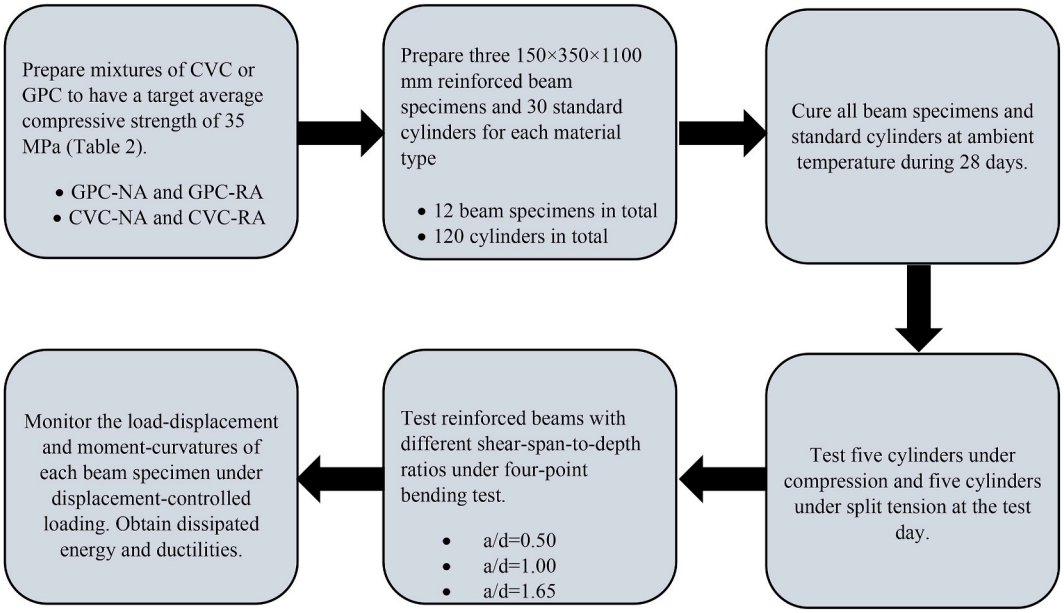

Fig. 5. Schematic of variables, curing procedures and mechanical tests.

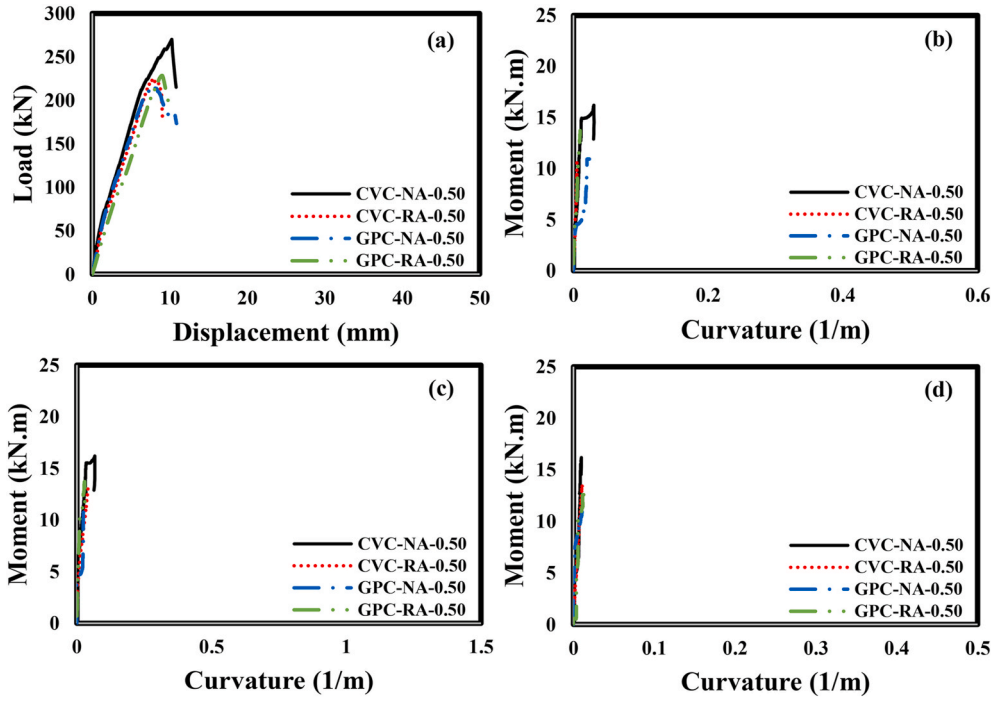

Fig. 6. Test Results of Beam Specimens with a/d = 0.50: (a) Total vertical load-midspan displacement, (b) the moment-curvature curve from left LVDTs, (b) the moment-curvature curve from mid-LVDTs, and (d) the moment-curvature curve from right LVDTs.

4.2. Test results of beam specimens with a/d = 1.00

The total vertical load-midspan displacement and the moment-curvature responses of CVC-NA-1.00, CVC-RA-1.00, GPC-NA-1.00, and GPC-RA-1.00 are given in Fig. 8. It could easily be inferred from Fig. 8 that the response of all specimens is less brittle than previous specimens. In these tests, it was observed that GPC specimens failed with a limited or no post-yield response due to less amount of flexure cracks at the midspan. However, CVC specimens showed a mixed shear-flexure failure, resulting in more ductility. This observation was also validated by the determined crack patterns (Fig. 9). The yield and ultimate loads, yield and ultimate displacements, and the ductility indices, are presented in Table 4.

4.3. Test results of beam specimens with a/d = 1.65

The total vertical load-midspan displacement and the moment-curvature responses of CVC-NA-1.65, CVC-RA-1.65, GPC-NA-1.65, and GPC-RA-1.65 are given in Fig. 10. It could easily be inferred from Fig. 10 that the response of all specimens is brittle. Limited or no post-yield response was observed. This observation was also validated by the determined crack patterns (Fig. 11). It is apparent from Fig. 11 that all

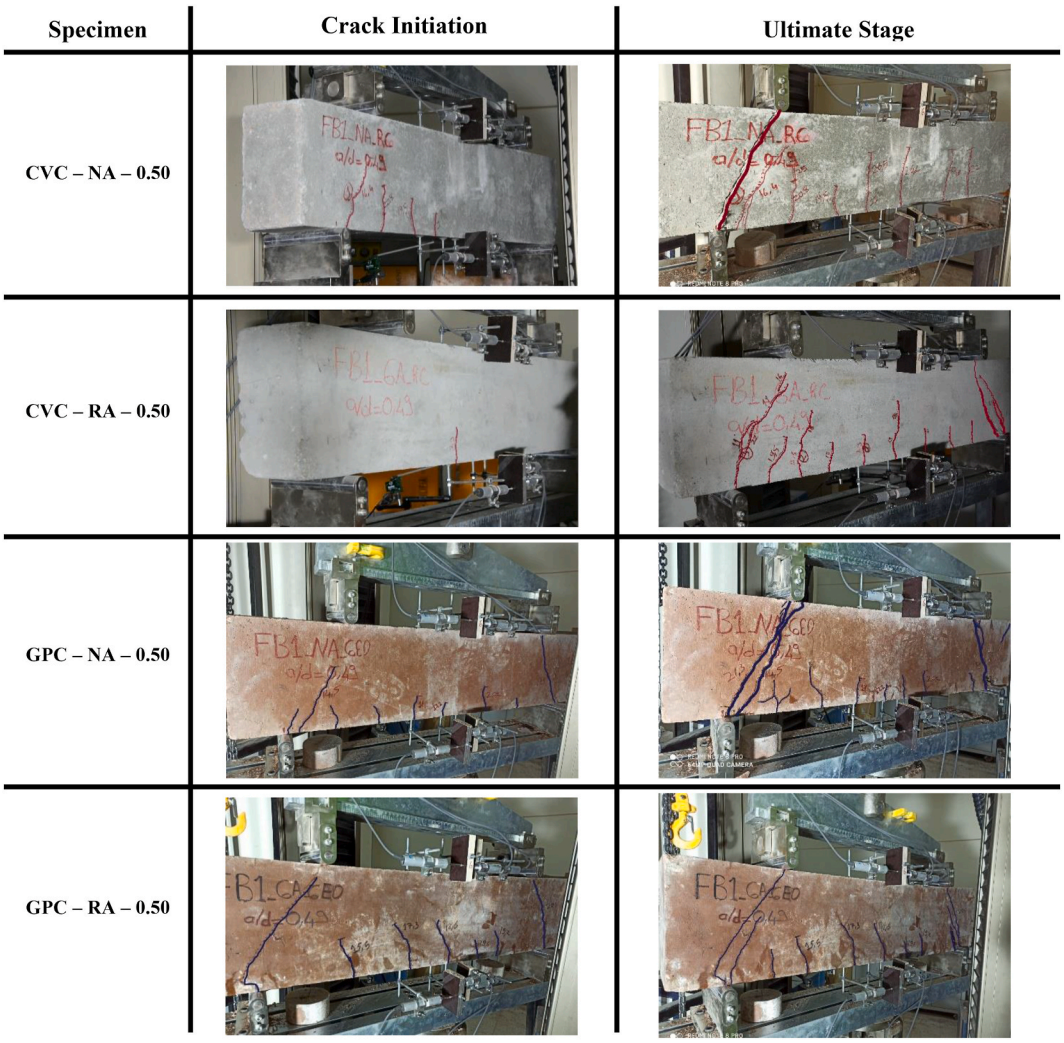

Fig. 7. Observed Crack Patterns of Beam Specimens with a/d = 0.50.

Table 4
Summary of test results.

Parameters	a/d = 0.50				a/d = 1.00				a/d = 1.65			
	CVC-NA	CVC-RA	GPC-NA	GPC-RA	CVC-NA	CVC-RA	GPC-NA	GPC-RA	CVC-NA	CVC-RA	GPC-NA	GPC-RA
F_y (kN)	230.11	204.51	205.85	220.08	165.10	168.81	165.98	170.06	99.16	98.91	99.08	99.18
F_u (kN)	270.05	224.46	216.82	228.58	180.40	183.63	184.68	189.66	112.08	102.11	105.04	103.5
M_y (kN.m)	NA	NA	NA	NA	18.26	16.18	18.91	19.65	18.86	16.49	19.89	18.96
M_u (kN.m)	16.20	13.46	13.00	13.71	22.10	22.49	23.23	21.85	19.91	20.48	20.18	20.18
u_y (mm)	10.09	11.60	8.20	12.00	9.16	11.25	11.16	10.45	9.16	8.16	9.81	9.96
u_u (mm)	13.18	13.63	14.11	15.5	20.89	27.91	26.18	21.78	39.81	26.63	37.68	26.02
φ_y (1/m)	NA	NA	NA	NA	0.03	0.03	0.03	0.03	0.11	0.09	0.10	0.10
φ_u (1/m)	NA	NA	NA	NA	0.13	0.11	0.12	0.10	0.96	0.65	0.98	0.72
μ_u	1.31	1.18	1.72	1.29	2.28	2.48	2.35	2.08	4.35	3.26	3.84	2.61
μ_φ	NA	NA	NA	NA	4.33	3.67	4.17	3.85	8.72	7.22	9.80	7.21
E_t (kN.m)	1.90	1.69	1.87	1.88	4.23	3.67	4.43	3.00	3.53	2.31	3.23	2.27
E_n	1.64	1.42	2.22	1.43	5.60	3.87	4.78	3.37	7.77	5.72	6.65	4.60

specimens failed by a shear – crack reaching the support. The yield and ultimate loads, yield and ultimate displacements, and the ductility indices, are presented in Table 4.

5. Analysis and discussion

5.1. Effect of material type

The performances of beam specimens with different material properties are discussed in this part. Firstly, it should be noted that the GPC-NA specimens had similar behavior to CVC-NA specimens as far as the load and displacement capacities were considered. This observation was

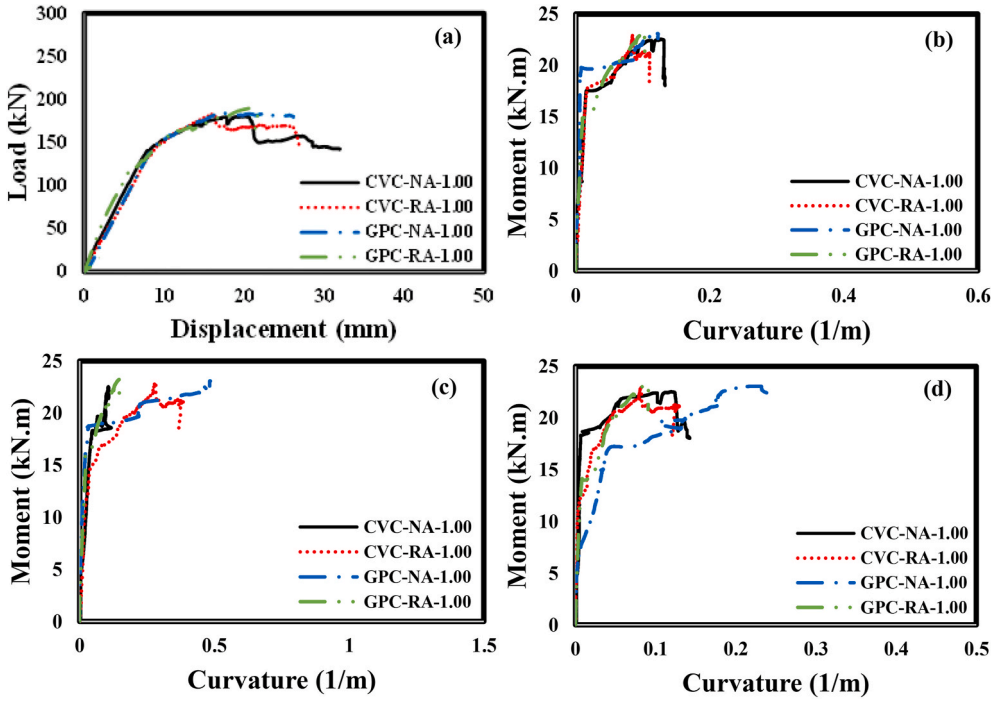

Fig. 8. Test Results of Beam Specimens with a/d = 1.00: (a) Total vertical load-midspan displacement, (b) the moment-curvature curve from left LVDTs, (b) the moment-curvature curve from mid LVDTs, and (d) the moment-curvature curve from right LVDTs.

also verified with the curvature capacities. Also, the cracks in these specimens showed similar patterns. Therefore, could easily be concluded that the proposed GPC mixture could perform as well as the CVC mixture.

However, the inclusion of recycled aggregates in the CVC and GPC mixtures resulted in a significant change in the behavior. Although the effect of recycled aggregate on the load capacities was negligible, this effect on the displacement capacities was substantial. For instance, the reduction in the ultimate displacement capacities of CVC and GPC specimens were 35% and 30%, respectively. In addition, a second observation was that the effect of recycled aggregates was more pronounced for flexure-dominated specimens (i.e., a/d = 1.65). This observation could be attributed to the secondary interfacial transition zone (ITZ) formation. Akbarnezhad et al. [53] claimed that the flexural ductility of beams depended on the bond strength between aggregate and paste. Since the most important factor affecting this bond strength is ITZ, a secondary ITZ formation was observed in mixtures with recycled aggregates due to formerly adhered mortar content surrounding the recycled aggregates. This secondary ITZ formation reduced the flexural capacity, postponing the shear cracks. This observation was also proved by comparing the flexural strengths of mixtures with and without recycled aggregates (Table 3). It was apparent from Table 3 that approximately a 10% reduction in the flexural strength of mixtures with recycled aggregates existed. It was, furthermore, known that the effect of ITZ depends significantly on the water/binder ratio of mixtures using recycled aggregates [54], and the relatively high water/binder ratio in the Portland cement beams and free water in geopolymer beams were expected to produce a weaker ITZ formation.

The recycled aggregates caused a significant reduction in the normalized energy dissipation capacities of CVC and GPC specimens. Independent from the different mixtures and different modes of failures, the reduction in the normalized energy dissipation capacities reached nearly 30% in the case of the replacement of normal aggregates with recycled aggregates. This observation underlined the similarities of CVC and GPC specimens in terms of flexural behavior.

5.2. *Effect of shear-span-to-depth ratio*

The first shear-span-to-depth ratio was selected as 0.50 to investigate the possible shear failure for these code-conforming beam specimens. As expected, all specimens, independent from the construction material chosen, failed in shear and showed brittle load-deflection and moment-curvature responses. Although the moment-curvature curves were not suitable to examine the behavior of reinforced concrete specimens due to the formation of inclined cracks between the load application point and the support, the change in the curvature response over the beam was also provided for the sake of completeness. It could easily be inferred from Fig. 6 that geopolymer concrete had very similar behavior compared to its conventional concrete counterparts in terms of load and deformation capacities. The failure patterns of all specimens were also detected to be similar (Fig. 7). This observation proved that, for shear-dominant behavior, i) the recycled aggregate had a very limited impact on the performance of concrete, and ii) the reinforced geopolymer concrete could perform nearly the same as conventional reinforced concrete if the shear-dominant behavior was investigated. In addition, the displacement and curvature ductilities of all specimens (i.e., CVC-NA-0.50, CVC-RA-0.50, GPC-NA-0.50, and GPC-RA-0.50) were determined to be very low (Table 4). The other observation was that the normalized energy dissipation capacities of all specimens with recycled aggregates were also less than other specimens without recycled aggregates (Table 4).

The second shear-span-to-depth ratio (i.e., a/d = 1.00) was used to determine the mixed shear-flexure failure for code-conforming reinforced beam specimens. All CVC specimens failed in shear-flexure combined action, manifesting itself by inclined cracks between the support and load application point and vertical cracks at the midspan. However, GPC specimens failed with a limited or no post-yield response due to fewer flexure cracks at the midspan. Unlike the first a/d ratio (i.e., 0.50), there exists some ductility, implied by the yield plateau in load-displacement and moment-curvature curves in Fig. 8. It should be stated that the mid LVDTs attached to specimens CVC-NA-1.00 and GPC-RA-1.00 stopped recording at a load value of 81 kN and 96 kN, respectively. Therefore, the curvature ductility comparisons of all

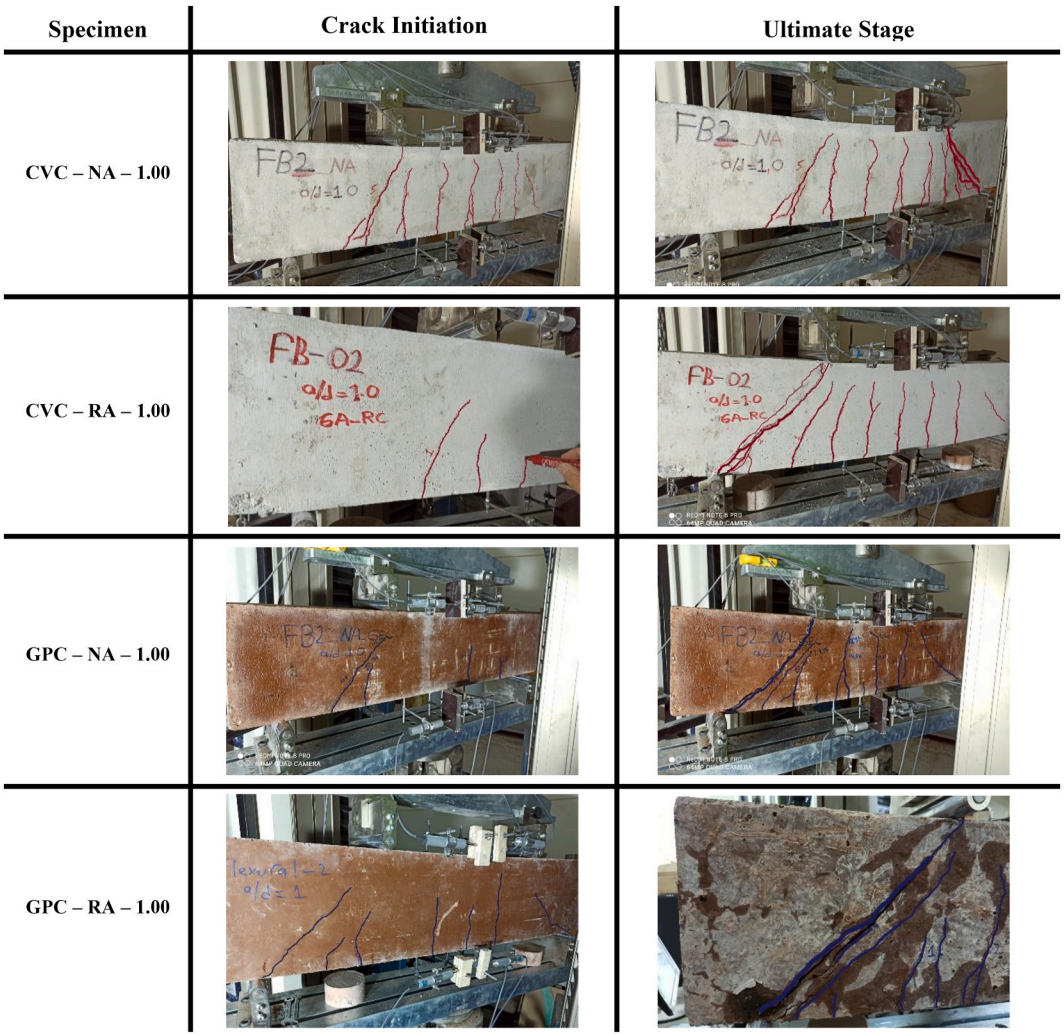

Fig. 9. Observed Crack Patterns of Beam Specimens with a/d = 1.00.

specimens were made by using left LVDTs. The curvature ductility values of each specimen ranged between 3.67 and 4.33. It was clear from Table 4 that geopolymer concrete had a curvature ductility of close to 4. If the curvature values determined from the mid LVDTs and left LVDTs were compared, the maximum curvature demand (i.e., mid LVDTs) at the midspan resulted in nearly three times the curvature demand at the left span (i.e., mid LVDTs). The reinforced geopolymer concrete could perform almost the same as the conventional reinforced concrete if the shear-flexure-dominant behavior was investigated. The other observation was that the normalized energy dissipation capacities of all specimens with recycled aggregates were also less than other specimens without recycled aggregates (Table 4). The decrease in normalized energy dissipation capacity for CVC and GPC specimens was 30.89% and 29.50%, respectively.

The last shear-span-to-depth ratio (i.e., a/d = 1.67) was utilized to study the flexure-dominant failure for code-conforming reinforced beam specimens with different materials. All specimens failed in flexure-dominant action, manifesting themselves by nearly vertical cracks concentrated at the midspan. In all of these tests, there exists a significant amount of ductility, implied by the large yield plateau in load-displacement and moment-curvature curves in Fig. 10. The curvature ductility comparisons of all specimens were made by using midspan LVDTs. The curvature ductility values of each specimen ranged between 7.21 and 9.80. It was clear from Table 4 that geopolymer concrete had a curvature ductility of close to 10, which is near twice the curvature ductility of specimens with an a/d ratio of 1.00. The failure patterns of all specimens were also detected to be similar (Fig. 11). This observation proved that the reinforced geopolymer concrete could perform nearly the same as the conventional reinforced concrete if the flexure-dominant behavior was investigated. However, the recycled aggregate had a negative effect on the performance of concrete, i.e., some reduction inductility and hence energy dissipation capacity was observed (Table 4).

The capacity estimation performances of two current codes: ACI318-19 [55] and TS500 [56], were also investigated in the scope of this study. The nominal shear capacity and the nominal moment capacities of each specimen were calculated by using proposed equations in ACI318-19 [55] and TS500 [56] and are presented in Table 5. In Table 5, the estimated capacity (V_{cap}) was obtained from the minimum of the nominal shear strength (V_n) and the ratio of nominal moment capacity (M_n) to moment arm. It could easily be inferred that the estimation performance of TS500 [56] is slightly better than the estimation performance of ACI318-19 [55]. It should also be noted that the estimation performance of codes is independent of the material type and the use of recycled aggregates. Besides, the estimation performance is slightly better for shear-dominant failures.

6. Conclusions

In this study, the structural properties of reinforced geopolymer concrete beams produced from 100% CDW-based materials were determined by performing laboratory experiments. In addition, the

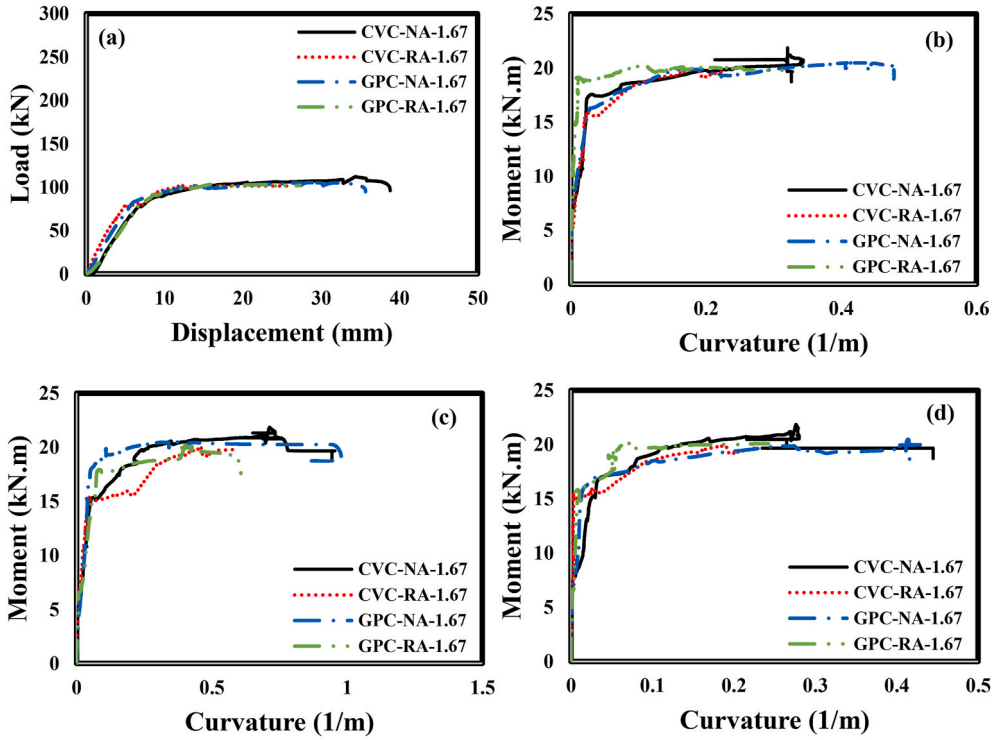

Fig. 10. Test Results of Beam Specimens with a/d = 1.65: (a) Total vertical load-midspan displacement, (b) the moment-curvature curve from left LVDTs, (b) the moment-curvature curve from mid-LVDTs, and (d) the moment-curvature curve from right LVDTs.

effect of the inclusion of recycled aggregate in the mixtures was investigated. To this end, bending tests were performed on reinforced conventional concrete beam specimens and reinforced geopolymer concrete beam specimens. Twelve specimens were tested to compare the structural behavior of geopolymer concrete beams with conventional concrete beams. The selected parameters in this study are three different shear-span-to-depth ratios and the inclusion of recycled aggregates in the concrete mixture. Therefore, the structural performance of beams was, firstly, compared for mixtures without recycled aggregates to control the possible side effects of 100% recycled concrete construction. Load-deflection curves, moment-curvature curves, and crack patterns were utilized to study the performance of geopolymer concrete. The following important conclusions can be drawn based on the results of the limited number of tests conducted in this study:

1 The GPC-NA specimens had similar behavior to CVC-NA specimens as far as the load and displacement capacities were considered. This observation was also verified with the curvature capacities. Also, the cracks in these specimens showed similar patterns.
2 The inclusion of recycled aggregates in the CVC and GPC mixtures resulted in a significant change in the behavior. Although the effect of recycled aggregate on the load capacities was negligible, this effect on the displacement capacities was significant (up to 30% difference). In addition, the effect of recycled aggregates was more pronounced for flexure-dominated specimens (i.e., a/d = 1.65). This observation could be attributed to the secondary interfacial transition zone (ITZ) formation.
3 The recycled aggregates caused a significant reduction in the normalized energy dissipation capacities of CVC and GPC specimens. Independent from the different mixtures and different modes of failures, the reduction in the normalized energy dissipation capacities reached nearly 30% in the case of the replacement of normal aggregates with recycled aggregates.
4 The geopolymer concrete had a significant amount of ductility if flexure-dominant behavior could be enforced on the designed structural element. The curvature ductility of geopolymer concrete was proven to be comparable to conventional concrete. Therefore, geopolymer concrete could be a possibly strong replacement candidate.
5 The failure patterns of all specimens were also detected to be similar except for shear-flexure dominant behavior. This implies that geopolymer concrete obeyed nearly the same failure surface.
6 The normalized energy dissipation capacities of all specimens with recycled aggregates were also less than other specimens without recycled aggregates. The decrease in normalized energy dissipation capacity for CVC and GPC specimens was approximately 30%. However, the recycled aggregate had a very limited impact on the load capacity.
7 The reinforced geopolymer concrete was similarly performed to the conventional reinforced concrete for especially flexure-dominated a/d ratios as far as the load capacity, displacement capacity, and energy dissipation capacity were considered. The percentage deviations for the listed parameters were all less than 10%.
8 The test observations clearly showed that construction demolition waste could be recycled to produce new constructional components, considering its advantage of promoted sustainability.
9 Code estimations failed to have low deviations and insignificant percentage errors. The percentage of errors reached as large as 45%. Although the authors are aware of the fact that the code formulations should result in conservative estimations, it should be noted that the code calculations in this study did not include the material factors. Therefore, the estimates should be reconsidered when the material and load factors are applied to them. The material factor along with the load factors, would result in a further reduction in the estimations in the order of approximately 2. Thus, the code estimations would give a factor of safety of around 4 for the tested specimens.

CRediT authorship contribution statement

Şaban Akduman: Testing. **Oznur Kocaer:** Writing – original draft.

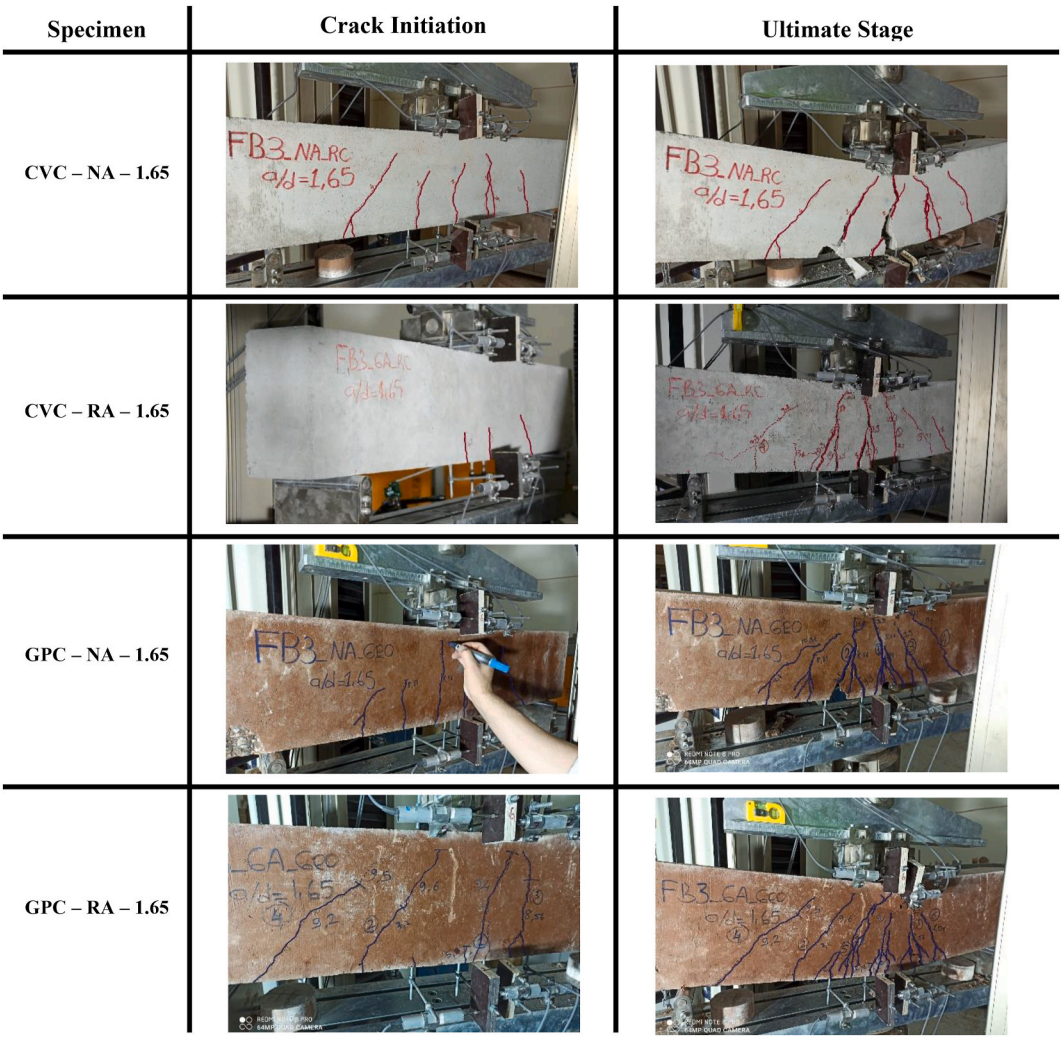

Fig. 11. Observed Crack Patterns of Beam Specimens with a/d = 1.65.

Table 5
Estimation performance of code proposed equations.

Specimens	Experiment			TS500 Estimations				ACI318-19 Estimations			
	M_{max} (kN.m)	F_{max} (kN)	V_{max} (kN)	M_n (kN.m)	V_n (kN)	V_{cap} (kN)	Error (%)	M_n (kN.m)	V_n (kN)	V_{cap} (kN)	Error (%)
CVC-NA-0.50	16.2	270.1	135.0	15	91.6	91.60	−32.15	12.7	89.2	89.2	−33.93
CVC-RA-0.50	13.5	224.5	112.2	15.1	96.5	96.50	−13.99	12.8	93.8	93.8	−16.40
GPC-NA-0.50	13.0	216.8	108.4	15	95.1	95.10	−12.27	12.8	92.5	92.5	−14.67
GPC-RA-0.50	13.7	228.6	114.3	15	94.6	94.60	−17.24	12.8	92.1	92.1	−19.42
CVC-NA-1.00	22.1	180.4	90.2	15	91.6	61.22	−32.12	12.7	89.2	51.84	−42.53
CVC-RA-1.00	22.5	183.6	91.8	15.1	96.5	61.63	−32.86	12.8	93.8	52.24	−43.09
GPC-NA-1.00	22.6	184.7	92.3	15	95.1	61.22	−33.67	12.8	92.5	52.24	−43.40
GPC-RA-1.00	23.2	189.7	94.8	15	94.6	61.22	−35.42	12.8	92.1	52.24	−44.89
CVC-NA-1.67	21.9	112.1	56.0	15	91.6	38.46	−31.32	12.7	89.2	32.56	−41.85
CVC-RA-1.67	19.9	102.1	51.1	15.1	96.5	38.72	−24.23	12.8	93.8	32.82	−35.77
GPC-NA-1.67	20.5	105.0	52.5	15	95.1	38.46	−26.74	12.8	92.5	32.82	−37.48
GPC-RA-1.67	20.2	103.5	51.8	15	94.6	38.46	−25.75	12.8	92.1	32.82	−36.64

Alper Aldemir: Conceptualization, Methodology, Writing – original draft. **Mustafa Şahmaran:** Funding acquisition, Project administration, Writing – review & editing. **Gürkan Yıldırım:** Writing – review & editing. **Hanady Almahmood:** Writing – review & editing. **Ashraf Ashour:** Funding acquisition, Writing – review & editing.

Declaration of competing interest

The authors declare that they have no known competing financial interests or personal relationships that could have appeared to influence the work reported in this paper.

Acknowledgments

The authors gratefully acknowledge the European Union's Horizon 2020 Research and Innovation Programme's financial assistance under Grant Agreement No: 869336 and Acronym: ICEBERG and the financial assistance of the Scientific and Technical Research Council (TUBITAK)

of Turkey and the British Council under Grant no:218M102. This work was also supported by Newton Prize 2020.

References

[1] K. Rashid, A. Razzaq, M. Ahmad, T. Rashid, S. Tariq, Experimental and analytical selection of sustainable recycled concrete with ceramic waste aggregate, Construct. Build. Mater. 154 (2017) 829–840.

[2] L.K. Turner, F.G. Collins, Carbon dioxide equivalent (CO2–e) emissions: a comparison between Geopolymer and OPC cement concrete, Construct. Build. Mater. 43 (2013) 125–130.

[3] J. De Brito, N. Saikia, Recycled Aggregate in Concrete: Use of Industrial, Construction and Demolition Waste, Springer Science & Business Media, 2012.

[4] K. Rashid, A. Yazdanbakhsh, M. Ul Rehman, Sustainable selection of the concrete incorporating recycled tire aggregate to be used as medium to low strength material, J. Clean. Prod. (2019).

[5] G. Yildirim, A. A Kul, E. Özçelikci, M. Sahmaran, A. Aldemir, D. Figueira, A. F. Ashour, Development of alkali-activated binders froRecycled mixed masonry-originated waste, Journal of Building Engineering 33 (2020) 101690.

[6] H. Ulugöl, A. Kul, G. Yıldırım, M. Şahmaran, A. Aldemir, D. Figueira, A.F. Ashour, Mechanical and microstructural characterization of geopolymers from assorted construction and demolition waste-based masonry and glass, J. Clean. Prod. (2020).

[7] J. Davidovits, Geopolymers: inorganic polymeric new materials, J. Therm. Anal. 37 (1991) 1633–1656.

[8] F. Pelısser, B.V. Sılva, M.H. Menger, B.J. Frasson, T.A. Keller, A.J. Torıı, R.H. Lopez, Structural Analysis of Composite Metakaolin-Based Geopolymer Concrete 11 (3) (2018) 535–543, 1983-4195.

[9] K.H. Mo, U.J. Alengaram, M.Z. Jumaat, Structural performance of reinforced geopolymer concrete members: a review, Construct. Build. Mater. 120 (2016) 251–264.

[10] P. Duxson, J.L. Provis, G.C. Lukey, J.S.J.V. Deventer, The role of inorganic polymer technology in the development of green concrete, Cement Concr. Res. 37 (12) (2007) 1590–1597.

[11] S. Kumar, J. Pradeepa, P.M. Ravindra, S. Rajendra, Flexural behavior of fly ash based reinforced geopolymer concrete beams, Int. J. Struct. Civil Eng. Res. 3 (No. 3) (August 2014), 2319 – 6009, www.ijscer.com.

[12] P.K. Mehta, Reducing the environmental impact of concrete, Concr. Int. 23 (10) (2001) 61–66.

[13] T.V. Madhava, G. Manjunath, K. Venugopal, Phenomenological model to Re-proportion the ambient cured geopolymer compressed blocks, Int. J. Concr. Struct. Mater. 7 (3) (2013) 193–202.

[14] A. Kar, I. Ray, U.B. Halabe, A. Unnikrishnan, B. Dawson-Andoh, Characterizations and quantitative estimation of alkali-activated binder paste from microstructures, Int. J. Concr. Struct. Mater. 8 (3) (2014) 213–228.

[15] K.T. Nguyen, T.A. Le, K. Lee, Experimental study on flexural strength of reinforced geopolymer concrete beams, Int. J. Civil Environ. Eng. 10 (No:4) (2016).

[16] S. Luhar, S. Chaudhary, I. Luhar, Development of rubberized geopolymer concrete: strength and durability studies, Construct. Build. Mater. 204 (2019) 740–753, https://doi.org/10.1016/j.conbuild mat.2019.01.185.

[17] D. Khale, R. Chaudhary, Mechanism of geopolymerization and factors influencing its development: a review, J. Mater. Sci. 42 (3) (2007) 729–746, https://doi.org/10.1007/s1085 3-006-0401-4.

[18] P. Duxson, J.L. Provis, G.C. Lukey, J.S.J. Van Deventer, The role of inorganic polymer technology in the development of 'green concrete', Cement Concr. Res. 37 (12) (2007) 1590–1597, https://doi.org/10.1016/j.cemco nres.2007.08.018.

[19] H.Q. Ahmed, D.K. Jaf, S.A. Yaseen, Flexural capacity and behaviour of geopolymer concrete beams reinforced with glass fibre-reinforced polymer bars, Int. J. Concr. Struct. Mater. (2020), https://doi.org/10.1186/s40069-019-0389-1.

[20] P.J.M. Monteiro, S.A. Miller, A. Horvath, Towards sustainable concrete, Nat. Mater. 16 (2017) 698–699.

[21] D.J. Flower, J.G. Sanjayan, Green house gas emissions due to concrete manufacture, Int. J. Life Cycle Assess. 12 (5) (2007) 282–288.

[22] U.S. Environmental Protection Agency (EPA). 2017. Advancing Sustainable Materials Management: 2017 Fact Sheet.

[23] AECOM Asia Company Limited. People's Republic of China: construction and demolition waste management and recycling. 2018.

[24] J. Davidovits, False values on CO2 emission for geopolymer cement/concrete published in scientific papers, Technical paper 24 (2015) 1–9 [c] Błaszczyński, T., & Król, M. (2015). Usage of green concrete technology in civil engineering. Procedia Eng., 122, 296-301.

[25] J. Liu, Z. Huang, X. Wang, Economic and environmental assessment of carbon emissions from demolition waste based on LCA and LCC, Sustainability 12 (16) (2020) 6683.

[26] J. Fort, E. Vejmelková, D. Koňáková, N. Alblová, M. Čáchová, M. Keppert, R. Černý, Application of waste brick powder in alkali activated aluminosilicates: functional and environmental aspects, J. Clean. Prod. 194 (2018) 714–725.

[27] M. Torres-Carrasco, F. Puertas, Waste glass in the geopolymer preparation. Mechanical and microstructural characterisation, J. Clean. Prod. 90 (2015) 397–408.

[28] N. Youssef, A.Z. Rabenantoandro, Z. Dakhli, F.H. Chehade, Z. Lafhaj, Environmental evaluation of geopolymer bricks, in: MATEC Web of Conferences, 281, EDP Sciences, 2019, p. 3005.

[29] D. Roy, Sulfoaluminate-belite cement from low-calcium fly ash and sulfur-rich and other industrial by-products, Cement Concr. Res. 29 (8) (1999) 1305–1311.

[30] J. Wongpa, K. Kiattikomol, C. Jaturapitakkul, P. Chindaprasirt, Compressive strength, modulus of elasticity, and water permeability of inorganic polymer concrete, Mater. Des. 31 (2010) 4748–4754.

[31] M.S. Badar, K. Kupwade-Patil, S.A. Bernal, J.L. Provis, E.N. Allouche, Corrosion of steel bars induced by accelerated carbonation in low and high calcium fly ash geopolymer concretes, Construct. Build. Mater. 61 (2014) 79–89.

[32] P. Chindaprasirt, T. Chareerat, S. Hatanaka, T. Cao, High-strength geopolymer using fine high-calcium fly ash, J. Mater. Civ. Eng. 23 (2010) 264–270.

[33] S. Zeng, J. Wang, Characterization of mechanical and electric properties of geopolymers synthesized using four locally available fly ashes, Construct. Build. Mater. 121 (2016) 386–399.

[34] P. Saravanakumar, Strength and durability studies on geopolymer recycled aggregate concrete, Int. J. Eng. Technol. 7 (2.24) (2018) 370–375.

[35] S.Kumaravel, S. Thirugnanasambandam, "Flexural Behaviour of Geopolymer Concrete Beams", Research paper E-ISSN2249–8974 (2013).

[36] M. Rajendran, N. Soundarapandian, An experimental investigation on the flexural behavior of geopolymer ferrocement slabs, J. Eng. Technol. 3 (2) (2013).

[37] R. Sanjay, M.U. Aswath, Smita Singh, An experimental study on flexural behaviour of reinforced geopolymer concrete beams with recycled aggregate in bending, Research Gate 6 (2) (2012), 2249-6149.

[38] S.D. Raj, N. Ganesan, R. Abraham, A. Raju, Behavior of geopolymer and conventional concrete beam column joints under reverse cyclic loading, Adv. Concr. Construct. 4 (No. 3) (2016) 161–172.

[39] Ahmed H. Q, Jaf D. K, Yaseen Ş. A, Flexural Capacity and Behaviour of Geopolymer Concrete Beams Reinforced with Glass Fibre-reinforced Polymer Bars.

[40] D.M.J. Sumajouw, D. Hardjito, S.E. Wallah, B.V. Rangan, Fly ash-based geopolymer concrete: study of slender reinforced columns, J. Mater. Sci. (2007).

[41] C. Wu, H. Hwang, C. Shi, N. Li, Y. Du, Shear tests on reinforced slag-based geopolymer concrete beams with transverse reinforcement, Eng. Struct. 219 (2020) 110966.

[42] G. Mathew, B. Joseph, Flexural behaviour of geopolymer concrete beams exposed to elevated temperatures, J. Build. Eng. 15 (2020).

[43] Turkish Earthquake Code (TEC2018), Specifications for the Buildings to Be Constructed in Disaster Areas, Prime Ministry Disaster and Emergency Management Authority, Ankara, Turkey, 2018.

[44] T.E. Azak, B.O. Ay, S. Akkar, A Statistical Study on Geometrical Properties of Turkish Reinforced Concrete Building Stock, in: 2nd European Conference on Earthquake Engineering and Sesimology, 2014. Istanbul, Turkey.

[45] E.G. Kurt, B. Binici, O. Kurc, E. Canbay, U. Akpinar, G. Ozcebe, Seismic performance of a deficient reinforced concrete test frame with infill walls, Earthq. Spectra 27 (3) (2011) 817–838.

[46] H. Sucuoglu, W. Lin, B. Binici, P. Ezzatfar, Pseudo-dynamic testing, performance assessment, and modeling of deficient reinforced concrete frames, ACI Struct. J. 111 (5) (2014) 1203–1212.

[47] T.K. Sipos, V. Sigmund, M. Hadzima-Nyarko, Earthquake performance of infilled frames using neural networks and experimental database, Eng. Struct. 51 (1) (2013) 113–127.

[48] B. Binici, E. Canbay, A. Aldemir, I.O. Demirel, U. Uzgan, Z. Eryurtlu, K. Bulbul, A. Yakut, Seismic behavior and improvement of autoclaved aerated concrete infill walls, Eng. Struct. 193 (2019).

[49] A. Aldemir, B. Binici, Y. Arici, O. Kurc, E. Canbay, Pseudo-dynamic testing of a concrete gravity dam, Earthq. Eng. Struct. Dynam. 44 (11) (2015) 1747–1763, https://doi.org/10.1002/eqe.2553.

[50] Y. Uchita, T. Shimpo, V. Saouma, Dynamic centrifuge tests of concrete dam, Earthq. Eng. Struct. Dynam. 34 (12) (2005) 1467–1487.

[51] V. Saouma, J. Broz, E. Brühwiler, H. Boggs, Effect of aggregate and specimen size on fracture properties of dam concrete, J. Mater. Civ. Eng. 3 (3) (1991) 204–218.

[52] Federal Emergency Management Agency (FEMA356), Prestandard and Commentary for the Seismic Rehabilitation of Buildings, 2000. Washington, DC.

[53] A. Akbarnezhad, K.C.G. Ong, M.H. Zhang, C.T. Tam, T.W.J. Foo, Microwave-assisted beneficiation of recycled concrete aggregates, Construct. Build. Mater. 25 (8) (2011) 3469–3479.

[54] N. Otsuki, S.I. Miyazato, W. Yodsudjai, Influence of recycled aggregate on interfacial transition zone, strength, chloride penetration and carbonation of concrete, J. Mater. Civ. Eng. 15 (5) (2003) 443–451.

[55] American Concrete Institute (ACI), Building code requirements, structural concrete and Commentary 318, ACI Committee, 2011.

[56] Turkish Standards (TS500), Design and Construction Rules of Reinforced Concrete Structures, Turkish Standards Institute, Ankara, Turkey, 2000.